

# Interpretation of the extensional modulus of oriented isotactic polypropylene using the aggregate and fibre composite models

A. P. Unwin, D. I. Bower and I. M. Ward\*

Department of Physics, University of Leeds, Leeds LS2 9JT, UK

(Received 2 March 1989; revised 2 October 1989; accepted 3 October 1989)

The extensional modulus of a series of uniaxially oriented tapes of isotactic polypropylene has been measured. The results are combined with earlier measurements of the orientation of the crystalline and non-crystalline regions and the reliability of several mechanical models is assessed. A single phase aggregate model, using the intrinsic mechanical properties of the crystal and overall measurements of orientation, is particularly successful in interpreting the low temperature mechanical moduli when the stress is assumed to be homogeneous throughout the material. At temperatures above the glass transition the distinction between the crystalline and non-crystalline components becomes significant and a two phase aggregate model provides better agreement with experimental results although its use is limited because of the number of unknown parameters and the possibility that the intrinsic mechanical properties of the non-crystalline phase may be sensitive to both temperature and orientation. Similarly, the number of unknown parameters limits the potential of a fibre composite model which provides good agreement with experiment at draw ratios greater than eight if a high fibre fraction is used. Such a high fraction would suggest identification of the fibre phase with either the microfibrils or helical sections of the molecule.

(Keywords: isotactic polypropylene; extensional modulus; mechanical properties)

## INTRODUCTION

One major problem has limited the success of model representations of the mechanical properties of semi-crystalline polymers; namely the identification of one or more of the different theoretical parameters with their experimentally measurable or morphological counterparts. Thus, for example, a simple Takayanagi model<sup>1</sup> in which the increase in modulus with draw ratio is attributed to an increase in the fraction of taut tie molecules, suffers from the absence of any reliable independent experimental measurements of this fraction. Another model is the aggregate model which considers the material to be composed of anisotropic units whose properties are identical to those of the fully oriented material. The macroscopic moduli are expressed in terms of the intrinsic mechanical properties of these units and their distribution of orientations within the sample. Although this model has been applied with some success to polyethylene and polypropylene<sup>2-6</sup>, there is no obvious morphological counterpart for the basic unit in a semicrystalline polymer.

More recently, following the interest in polymer composites, a fibre composite approach has been examined. In their model, Barham and Arridge<sup>7</sup> consider what happens in the post necking region of a semi-crystalline polymer and attribute the increase in modulus with draw ratio in this region to an increase in the aspect ratio of the reinforcing fibre phase, the concentration of which is assumed constant throughout the post neck drawing region. In a series of papers Barham and Arridge<sup>7-9</sup> used this model to interpret the mechanical properties of

polyethylene and polypropylene and obtained considerable success when values for the post neck fibre fractions were assumed. Again, however, there were no independent measurements of the fibre fractions. An alternative fibre composite approach, described by Gibson *et al.*<sup>10</sup>, has been more successful in overcoming this basic problem, but has only proved fruitful for polyethylene, where the increase in modulus is attributed to an increase in the degree of crystal continuity, the fibre phase being lengths of molecule bridging the non-crystalline regions. Experimental measurements of long period and crystal size strongly supported this interpretation. Recent work by Taraiya *et al.*<sup>11</sup> suggests that this specific intercrystalline bridge model is not suitable for polypropylene.

Some attempts to relate the mechanical properties of drawn polypropylene to the observed structural and intrinsic properties of the constituent phases using a modification of the aggregate model have been described by Samuels and co-workers<sup>12,13</sup> but their analysis uses intrinsic mechanical parameters which have not been determined independently. A similar argument applies to the work of Leung *et al.*<sup>14</sup>. Nevertheless, an important conclusion to be drawn from these attempts is that the orientation of the non-crystalline material can be important in determining the modulus. This conclusion has been further supported by the work of Yamada *et al.*<sup>15</sup>, who showed that the room temperature modulus of a series of samples with similar crystallinities and crystallite orientations, prepared in different ways, was related to the orientation of the non-crystalline material.

Overall, there is a lack of sufficient independent information to permit the adoption of a preferred model to describe the mechanical behaviour of polypropylene. Nevertheless, it is of specific interest to the understanding

\* To whom correspondence should be addressed

of the mechanical behaviour of polypropylene to assess the merits of the different models, and it is to this end that the present work is directed. This paper follows an earlier report<sup>16</sup> of the measurement of orientation in a series of drawn isotactic polypropylene tapes, and presents the results of mechanical measurements on the same series. In addition, the crystal modulus has been measured using an X-ray method and the models described above are assessed in the light of the results.

## THEORETICAL MODELS

### The aggregate model

In its simplest form this model, discussed by Ward<sup>2</sup>, assumes that the polymer is composed of an aggregate of many identical transversely isotropic units, each with mechanical properties identical to those of a fully oriented sample. The properties of the bulk sample are found by suitable averaging of the contributions from each microscopic unit, with due regard for its orientation. More specifically they can be expressed in terms of the moment averages of the orientation distribution function and the properties of the basic unit. The relation between the macroscopic mechanical properties and extension is often found by assuming a pseudo-affine deformation scheme to predict the moment averages. Alternatively the moment averages can be determined experimentally and the macroscopic properties predicted using the model.

The aggregate model, in its simplest form, does not directly consider how the differently oriented microscopic units are coupled to one another, but proposes two alternative averaging schemes. The first, which is usually assumed to mark the upper bound to the macroscopic moduli, is obtained by taking the ensemble average of the moduli of the basic units (the Voigt average, uniform strain), whilst the second, assumed to mark the lower bound, is obtained by applying the averaging process to the compliance constants, (the Reuss average, uniform stress).

Application of the aggregate model has met with some success, and it has been shown that for most polymers the Reuss average provides the better agreement. For Reuss averaging, the extensional compliance,  $S_{33}$ , (reciprocal of Young's modulus) of a transversely isotropic sample can be written<sup>2</sup>

$$S_{33} = \langle \sin^4 \theta \rangle s_{11} + \langle \cos^4 \theta \rangle s_{33} + \langle \sin^2 \theta \cos^2 \theta \rangle (2s_{13} + s_{44}) \quad (1)$$

where the  $s_{ij}$  are the components of the compliance matrix for the microscopic unit and are usually obtained from measurements on highly oriented samples. The angle  $\theta$ , is the inclination of the principal axis of symmetry of a unit to the draw direction, and the brackets,  $\langle \rangle$ , indicate an average value for all units, taken over the distribution of orientations.

A natural extension of this model to cover semi-crystalline polymers considers the properties of the two phases separately. In this case two basic units are considered, one with the properties of the crystalline phase, the other with the properties of the non-crystalline phase and the macroscopic modulus is found by averaging the compliances of the two phases. Thus the macroscopic compliance is given by

$$S_{33} = \beta S_{33}^c + (1 - \beta) S_{33}^a \quad (2)$$

where  $S_{33}^p$  for the phase  $p$  is obtained from equation (1) using the relevant parameters, and  $\beta$  is the crystallinity. The superscripts  $c$  and  $a$  refer to the crystalline and non-crystalline material, respectively. It is obvious that independent measurements of the properties of the two phases are particularly desirable, but although the mechanical properties of the crystal can be estimated from theory and experiment, those of the non-crystalline regions are not so easily obtained.

### The fibre composite model

One version of this model, described by Barham and Arridge<sup>7</sup>, considers the polymer to consist of crystalline rods or fibrils in a basically amorphous matrix, although the matrix may also contain some crystalline material. It assumes that the fibrils carry only the tensile stresses and the matrix, in which they are embedded, carries no tensile stress but transfers load from fibril to fibril by shear. For such a model they showed that the Young's modulus,  $E$ , of the sample is given by

$$E = cE_f(1 - \tanh x)/x + (1 - c)E_m \quad (3)$$

where  $E_f$  and  $E_m$  are the Young's moduli of the fibril and matrix respectively, and  $c$  is the volume concentration of the fibrils. The parameter  $x$  is given by

$$x = 2A[G_m/E_f \ln(2\pi/\sqrt{3c})]^{1/2} \quad (4)$$

where  $A$  is the aspect ratio (length/diameter) of the fibrils and  $G_m$  the shear modulus of the matrix.

The model attempts to explain the increase in modulus above the necking region, where it is assumed that there is no further change in orientation. It assumes that the needle-like fibrils deform homogeneously during drawing, increasing their length by the post neck draw ratio  $t$ . For constant volume deformation the aspect ratio at draw ratio  $t$ ,  $A_t$ , is then given by

$$A_t = A_0 t^{3/2} \quad (5)$$

where  $A_0$  is the aspect ratio of the fibrils in the undeformed fibrillar material ( $t=1$ ), i.e. at the end of necking. Equations (3), (4) and (5) give the dependence of the modulus on the post neck draw ratio. The main problem with this approach is that it is difficult to envisage how the relatively stiff fibrils can deform in a soft matrix and retain a constant  $E_f$ .

Gibson *et al.*<sup>10</sup> also considered a fibre composite model, but their physical interpretation of the nature of the reinforcing fibre phase differs from that of Barham and Arridge<sup>7</sup>. In the model of Gibson *et al.* the reinforcing elements are assumed to be the short lengths of polymer which cross one or more regions of non-crystalline material, thus producing a continuous crystalline phase. They do not envisage the reinforcing elements as discrete identifiable entities, which retain their identity throughout the drawing process, but prefer to consider that at each stage of deformation there is a degree of crystal continuity which can be represented by an apparent fibrillar content.

A further feature of the composite model is its ability to predict the dependence of Young's modulus on temperature. Thus, equations (3) and (4), combined with a knowledge of the dependence of the shear modulus on temperature, can be used to find Young's modulus as a function of temperature. This more promising aspect of the fibre composite model has been discussed by Gibson *et al.*<sup>17</sup>.

## EXPERIMENTAL

The samples used in this work were tapes of isotactic polypropylene (IPP) (HF-18, Imperial Chemical Industries Ltd) containing 0.004% of a fluorescent probe. Full details of the preparation of these tapes, together with measurements of orientation, have been reported elsewhere<sup>16</sup> and reference should be made there for detailed information. Briefly, drawn tapes were produced in one of two ways. Draw ratios in the range 1 to about 7 were produced by a continuous drawing method, in which isotropic tape ( $M_w \sim 450\,000$ ) was drawn between two rollers, running at different speeds, on a draw frame. To localize the draw point the tape passed round a roller (called the pin) immersed in glycerol at 110°C. Tapes produced in this way form series A. Samples in series B had draw ratios in the range 8 to 13 and were produced by drawing dumbbells cut from film ( $M_w \sim 330\,000$ ) on an Instron tensile testing machine at an air temperature of 110°C using a draw speed of 5 cm min<sup>-1</sup>. This corresponds to an initial strain rate of about 2 min<sup>-1</sup>.

### Mechanical measurements

Two types of macroscopic mechanical moduli are considered here. The 10 s isochronal creep modulus can be readily compared with earlier measurements of mechanical moduli on similar samples and is useful in this respect. Measurements of dynamic modulus provide a means of assessing molecular mobility which is of considerable significance in justifying subsequent modelling.

### Ten second isochronal creep modulus

Measurements of Young's modulus were made at room temperature using apparatus and method similar to that described by Gupta and Ward<sup>18</sup>. The creep strain at 10 s was measured as a function of applied load for a series of loads so that the load required to produce 0.1% strain could be found. The 10 s isochronal creep modulus at 0.1% strain could then be calculated when the cross sectional area of the sample had been measured.

### Dynamic modulus

Dynamic mechanical measurements were performed over an extensive temperature range at frequencies of 1 and 10 Hz on samples of length about 5 cm mounted in tension between two stainless steel clamps. A sinusoidal extension was applied to the sample by means of a vibrator driven by a Solatron 1250 frequency response analyser (FRA). A fuller description of the apparatus is given elsewhere<sup>19,20</sup> but the basic advantage of the FRA is the direct determination of the complex modulus through calculations of the ratio of the stress and strain signals. Calculations were performed by the FRA over several cycles and accepted if the variation was less than 5%. Occasionally the presence of lateral vibrations at particular temperatures and frequencies produces noisy results. The use of two different dynamic frequencies assists the identification of errors from this source.

The measurements were made with the samples under a dead load sufficient to produce a strain of about 0.15%. The oscillatory strain was held constant at 0.1% (peak to peak). Moduli determined using dead loads which produced strains of 0.1 and 0.2%, differed by less than 5%. The modulus was measured at temperatures accurate to 0.2°C in the range -100 to 70°C. Final values of modulus are accurate to about 8%.

### Crystal modulus

The crystal modulus of a sample can be obtained from measurements of the crystal strain, produced by the application of a known stress to the sample, if the stress can be regarded as transferred to the crystalline phase (i.e. the stress is homogeneous throughout the specimen). The crystal strain can be measured by observing the change in the diffraction angle,  $2\theta$ , for a suitable diffraction peak. For measurements in this work the ( $\bar{1}13$ ) reflection from a sample of draw ratio 11.7 was considered.

Copper K $\alpha$  radiation was obtained from a Siemens X-ray tube using a nickel filter. The active area of a position-sensitive detector lay on a chord of a circle, whose centre coincided with that of a standard Philips X-ray diffractometer table. The position sensitive detector was interfaced to a Norland Ino-Tech 5300 multichannel analyser, so that the multichannel analyser recorded the diffracted X-ray intensity along the chord, and consequently enabled the  $2\theta$  profile of the peak to be observed directly.

Measurements were performed on a single tape, which was mounted on a stretching rig consisting of two clamps mounted on a system of low friction linear bearings. One clamp was fixed and a dead load could be applied to the other in order to apply a constant stress to the sample, which was mounted between these two clamps. The sample was mounted so that the draw direction and the normal to the plane of the sample lay in the same plane as the incident and diffracted X-ray beams. The inclination of the sample draw direction to the bisector of the incident and diffracted X-ray beams was selected to give maximum intensity at the detector. The  $2\theta$  profile of the diffracted X-ray peak was then recorded for a series of applied dead loads, as well as for the unstressed state between each applied load. To obtain the central position of each peak, a fit of the experimental data to a theoretical curve, composed of a Gaussian peak, Lorentzian peak and a linear background was performed. The shift in position of the peak was used to calculate the change in the interplane spacing for the ( $\bar{1}13$ ) reflection, and this was then corrected to produce the strain in the  $c$  axis direction. Although IPP has a monoclinic crystal structure the deviation from orthorhombic structure is small and this correction can therefore be found quite accurately by assuming an orthorhombic structure and differentiating the interplane spacing with respect to the  $a$ ,  $b$  and  $c$  cell dimensions to obtain the relation between strains in the different directions. This has the added advantage that Poisson's ratio effects can easily be included. The correction factor for the ( $\bar{1}13$ ) plane is 0.89 without considering Poisson's ratio effects and 0.86 for a Poisson's ratio of 0.33. The crystal modulus was measured at two temperatures, -50°C and 20°C.

## RESULTS

Values for the room temperature Young's modulus in the draw direction, obtained from the ten second isochronal creep measurements, are tabulated in *Table 1*; *Figure 1* illustrates the variation with draw ratio. Initially there is a gradual increase in the modulus but above a draw ratio of 5 the modulus rises more rapidly, with a tenfold increase over the isotropic value being shown by samples of draw ratio 11. This behaviour, similar to that published elsewhere, was generally found to be poorly described by the aggregate model<sup>3-5</sup>.

**Table 1** Extensional modulus results for drawn IPP

Draw ratio	10 s creep modulus at room temperature	Dynamic modulus at 1 Hz and	
		-90°C (GPa)	45°C (GPa)
1	0.9	-	-
1.22	-	5.11	1.42
1.3	1.3	-	-
1.92	1.5	-	-
3.5	2.4	10.83	2.98
4.8	3.6	12.59	4.52
7.1	6.0	14.72	5.57
9.5	-	19.14	9.73
9.8	9.4	-	-
12.0	-	21.82	12.22
12.1	-	25.56	14.62
12.6	11.2	-	-

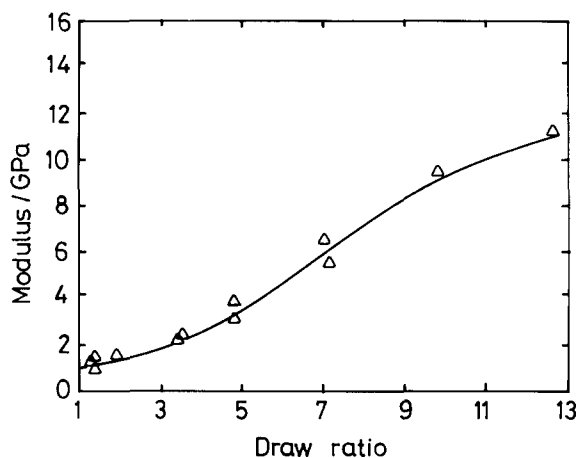
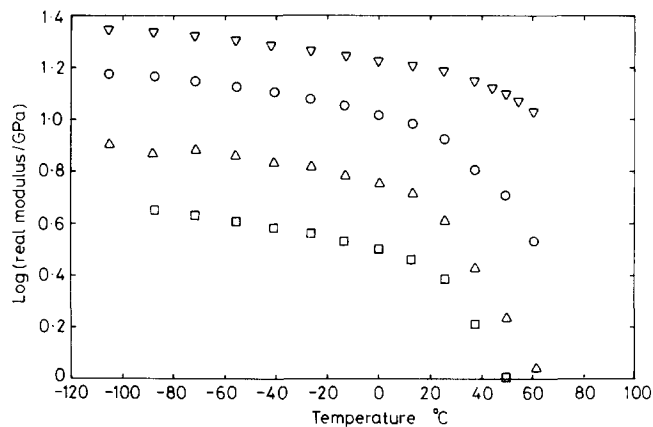
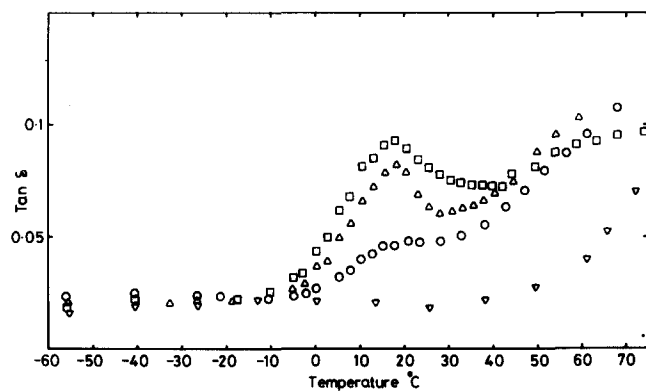
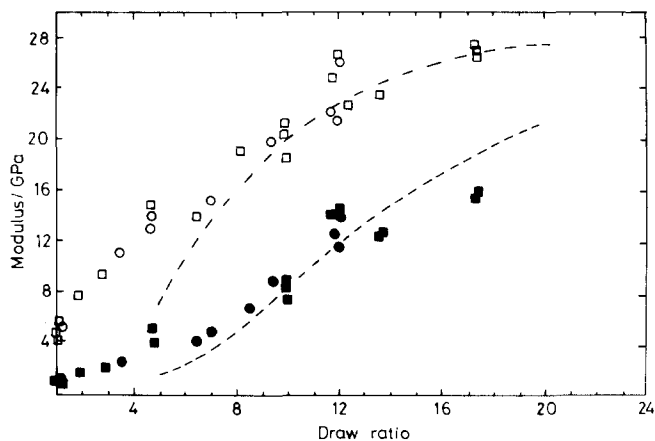

**Figure 1** Variation of 10s isochronal creep modulus at room temperature with draw ratio for IPP

Figure 2 shows the temperature dependence of the dynamic modulus of several samples, and Figure 3 the  $\tan \delta$  curves for the same samples. In each case the modulus increases as the temperature decreases, but rises much more slowly at low temperatures. Although there is still a small rise in modulus as the temperature decreases it is convenient to use the term 'plateau modulus' in the temperature region below about 0°C. This plateau value depends on the extension, being greater for higher draw ratios. The dependence of the modulus on draw ratio will be considered at two temperatures, one each side of  $T_g$ , the glass transition temperature (about 15°C). As expected, results at 10 Hz are slightly greater than those at 1 Hz and the same temperature, but the difference is small enough to allow both sets to be included in the modelling without introducing significant errors.

Some typical dynamic modulus results at temperatures of 45 and -95°C are listed in Table 1, and Figure 4 illustrates the variation with draw ratio. Immediately it can be seen that at low extensions (draw ratio < 5), the dependence of the modulus on draw ratio at 45°C is very different from that at -95°C. At a temperature of 45°C the modulus shows a small change with draw ratio and is in good agreement with the results obtained for the isochronal creep modulus. At -95°C, however, the modulus is much more sensitive to draw ratio at low extension.

Values of  $34 \pm 2$  GPa and  $35 \pm 2$  GPa were obtained for the longitudinal crystal modulus at 20°C and -50°C

respectively. These agree well with a value of 35 GPa, reported by Sakurada and Kaji<sup>21</sup>, although other authors have quoted slightly different values. Fanconi and Rabolt<sup>22</sup> have quoted a value as high as 88 GPa, but most other reports quote significantly lower values, and a theoretical calculation by Tashiro *et al.*<sup>23</sup> yielded a value of 25 GPa. The quoted errors of 6% in the present results arise principally from uncertainties in the gradient of the peak shift *versus* applied load graph and the sample cross-sectional area. In the event of non-homogeneous stress transfer within the sample the values reported here


**Figure 2** Temperature dependence of the dynamic modulus at 10 Hz for drawn samples of IPP.  $\square$ ,  $\lambda = 1$ ;  $\triangle$ ,  $\lambda = 1.92$ ;  $\circ$ ,  $\lambda = 4.8$ ;  $\nabla$ ,  $\lambda = 11.9$ 

**Figure 3** Temperature dependence of  $\tan \delta$  at 10 Hz for drawn samples of IPP. Symbols as in Figure 2

**Figure 4** Variation of dynamic modulus with draw ratio for frequencies,  $\circ$ , 1 Hz and  $\square$ , 10 Hz. Open points are for a temperature of -95°C and closed points for a temperature of 45°C. The dotted lines are fits predicted by the fibre composite model

would of course be underestimates. This possibility is discussed in detail later. Finally the crystallinity, measured using a density technique, was found to be typically about 58%.

## MODELLING

### Single phase aggregate model

We will first compare the predictions of the single phase model with the low temperature ( $-95^{\circ}\text{C}$ ) dynamic modulus results. The components of the compliance matrix which are used here are those for the crystalline phase,  $s_{ij}^c$ . This has particular merit since the values of these quantities are the most readily obtainable. A value of  $s_{33}^c = 0.029 \text{ GPa}^{-1}$  is obtained from the measurements of the crystal modulus. A value of  $0.33 \text{ GPa}^{-1}$  for  $s_{11}^c$  has been quoted by Sakurada *et al.*<sup>24</sup>, but unfortunately there is no information for the term  $(2s_{13}^c + s_{44}^c)$ . An estimate of its value, however, may be found by considering the modulus of a totally random sample. Substitution of the above values into equation (1) gives a value of  $0.41 \text{ GPa}^{-1}$  for  $(2s_{13}^c + s_{44}^c)$ .

Alternatively if Poisson's ratio,  $\nu = -s_{13}/s_{33}$ , is assumed to be 0.35, and the low temperature shear modulus<sup>25</sup> is used to give a value for  $s_{44}^c$  of  $0.59 \text{ GPa}^{-1}$  the value of the parameter  $(2s_{13}^c + s_{44}^c)$  is found to be  $0.4 \text{ GPa}^{-1}$ , which agrees well with the value given above.

For the pseudo-affine deformation scheme the orientation parameters in equation (1) can be obtained from the draw ratio in the manner described by Ward<sup>2</sup>. Figure 5 shows the predicted variation in modulus as a function of draw ratio using the above values for  $s_{ij}^c$  and assuming a pseudo-affine deformation. The curves for both Reuss and Voigt averaging are given, although in the absence of a complete knowledge of the compliance matrix, approximate values for the stiffness constants have been obtained from the reciprocal compliance values. Also shown in Figure 5 are two additional Reuss curves using considerably different values of  $(2s_{13}^c + s_{44}^c)$  as well as the results of modulus measurements at  $-95^{\circ}\text{C}$  on the drawn IPP samples. Birefringence measurements<sup>16</sup> on these samples have shown that the overall deformation is

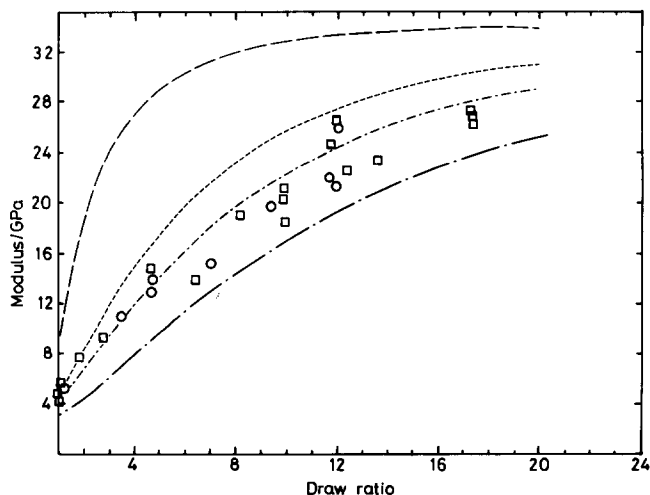


Figure 5 Comparison of dynamic modulus results at  $-95^{\circ}\text{C}$  with the single phase aggregate model. —, Voigt averaging; ---, Reuss averaging for  $(2s_{13}^c + s_{44}^c) = 0.41 \text{ GPa}^{-1}$ ; Reuss averaging for  $\dots$ ,  $(2s_{13}^c + s_{44}^c) = 0.17 \text{ GPa}^{-1}$ ; and - · - ·,  $(2s_{13}^c + s_{44}^c) = 1 \text{ GPa}^{-1}$ . Values for the other constants are given in the text

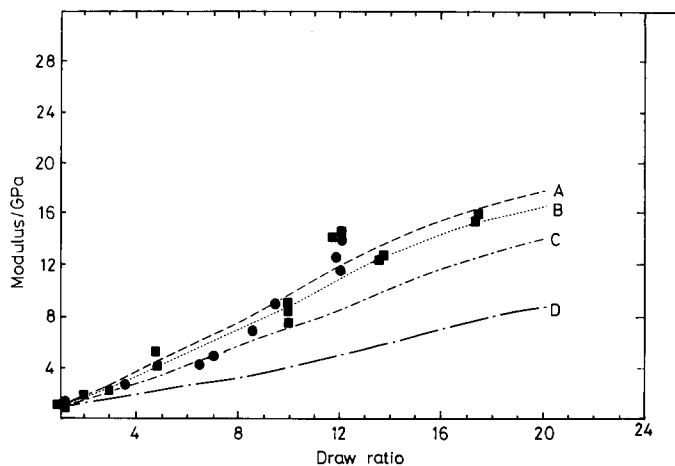


Figure 6 Comparison of modulus results at  $45^{\circ}\text{C}$  with two phase aggregate model using Reuss averaging. ---, A,  $s_{11}^a = 2.5 \text{ GPa}^{-1}$ ;  $(2s_{13}^a + s_{44}^a) = 0.41 \text{ GPa}^{-1}$ ;  $\dots$ , B,  $s_{11}^a = 2.38 \text{ GPa}^{-1}$ ;  $(2s_{13}^a + s_{44}^a) = 1.0 \text{ GPa}^{-1}$ ; - · - ·, C,  $s_{11}^a = 2.0 \text{ GPa}^{-1}$ ;  $(2s_{13}^a + s_{44}^a) = 2.5 \text{ GPa}^{-1}$ ; —, D,  $s_{11}^a = 0.33 \text{ GPa}^{-1}$ ;  $(2s_{13}^a + s_{44}^a) = 9.18 \text{ GPa}^{-1}$

pseudo-affine. Clearly there is remarkably good agreement between the predicted and experimental results at  $-95^{\circ}\text{C}$  when Reuss averaging is considered. Furthermore, the effect of altering considerably the only unknown parameter,  $(2s_{13}^c + s_{44}^c)$ , is not to change significantly the predictions of the model.

### Two phase aggregate model

The predictions of the two phase model will be compared with the dynamic modulus results at  $45^{\circ}\text{C}$ . The values of the compliance constants for the crystal phase,  $s_{ij}^c$ , are taken to be those used above in the single phase model. Unfortunately it is not possible to measure directly the compliance constants for the non-crystalline phase,  $s_{ij}^a$ , so several approximations need to be made. It has been shown<sup>26</sup> that the molecules in the amorphous phase can be regarded as short helical sections separated by conformational reversals. Because the intermolecular forces are considerably weaker than the intramolecular forces it is reasonable to assume that  $s_{33}^a = s_{33}^c$ . Values for the other non-crystalline parameters,  $s_{11}^a$  and  $(2s_{13}^a + s_{44}^a)$ , are obtained from the modulus of a random sample using equations (1) and (2) with a value of 0.58 for  $\beta$ . These two parameters are the only unknowns and so a series of pairs of values for them will satisfy equation (2) for an isotropic sample. The dynamic modulus at  $45^{\circ}\text{C}$  of the undrawn sample was used to provide these values. Considering only the case of Reuss averaging the possible pairs of values for these parameters predict moduli that fall between two bounds. The lower Reuss bound to the modulus is given by having  $s_{11}^a = s_{11}^c$ , whilst the upper Reuss bound is given by having  $(2s_{13}^a + s_{44}^a) = (2s_{13}^c + s_{44}^c)$ . These two cases predict values of  $(2s_{13}^a + s_{44}^a) = 9.18 \text{ GPa}^{-1}$  and  $s_{11}^a = 2.5 \text{ GPa}^{-1}$ , respectively. Two additional intermediate sets of values were arbitrarily chosen, namely  $s_{11}^a = 2 \text{ GPa}^{-1}$ ,  $(2s_{13}^a + s_{44}^a) = 2.5 \text{ GPa}^{-1}$  and  $s_{11}^a = 2.4 \text{ GPa}^{-1}$ ,  $(2s_{13}^a + s_{44}^a) = 1 \text{ GPa}^{-1}$ . The values for the orientation parameters were obtained using the X-ray measurements reported earlier<sup>16</sup> and assuming that the contributions of the different phases to the orientation functions averaged to produce pseudo-affine values.

Figure 6 shows the predicted curves for Reuss averaging plus the experimental points at  $45^{\circ}\text{C}$ . Good agreement

between the predicted and experimental results is obtained when the value of  $(2s_{13} + s_{44})$  is the same for both phases (curve A), an agreement which is not repeated when the restriction is applied to  $s_{11}$  (curve D). In reality both  $s_{11}^a$  and  $(2s_{13}^a + s_{44}^a)$  would be expected to be greater than  $s_{11}^c$  and  $(2s_{13}^c + s_{44}^c)$  respectively, and the Reuss curve for this situation should fall between the limits A and D.

#### The fibre composite model applied to IPP

As mentioned earlier, there are two aspects of the fibre composite model worthy of attention; namely the dependence of the modulus at a fixed temperature on affine deformation of the fibrils and the dependence of the modulus on temperature. Of these, the former will be considered first because fewer parameters are needed. The fibril modulus is assumed to be equal to the crystal modulus, 35 GPa, and this value, coupled with the sample modulus, restricts the possible range of  $c$  if  $E_f \gg E_m$ , which initially is assumed to be so. If the model is applied at low temperatures where the sample modulus can be greater than 28 GPa, a  $c$  value greater than 0.8 is required. Thus  $(1-c)$  is close to zero, and this together with the small value for  $E_m$  means that the second term on the right hand side of equation (3) can be neglected to a first approximation.

It is not necessary to know explicitly a value for the parameter  $x$  in order to assess the merits of this model. Instead, if a value is assumed for  $c$ , equation (3) can be used to calculate the value of  $x$  required to produce a certain macroscopic modulus. This procedure was followed for an arbitrarily chosen fibril concentration of 0.9 and a sample modulus of 21 GPa, which corresponds to the low temperature modulus of a sample of  $\lambda = 10$ . For affine deformation of the fibrils equations (4) and (5) show that the ratio of the values of  $x$  at two different draw ratios is given by

$$x_1/x_2 = [t_1/t_2]^{1.5} = [\lambda_1/\lambda_2]^{1.5} \quad (6)$$

Values for  $x$  at different draw ratios,  $\lambda$ , were thus obtained without the need to know the aspect ratio, shear modulus or even the true post neck draw ratio. The variation of modulus, thus predicted, is shown in *Figure 4*, where good agreement with the low temperature data is observed except for values of  $\lambda$  less than about 8. This suggests that a draw ratio of 8 marks the completion of the spherulitic to fibrillar transition. It is worth noting at this point that measurements of orientation on samples prepared using the two different drawing routes showed no discontinuity at the cross over draw ratio ( $\sim 8$ ), although it is of course possible that the morphology is discontinuous at this boundary. The assumption of a morphological change is implicit in the fibre composite model and it is not possible to eliminate the different drawing processes as a possible reason for this change.

A  $c$  value of 0.8 provides a better fit to the low draw ratio samples but results in greater discrepancies at high draw ratios. Lower values of  $c$  do not improve the fit unless the contribution from  $E_m$  is no longer considered negligible. It is interesting to note that a  $c$  value of 0.907 corresponds to close hexagonal packing of cylinders of equal diameter. Thus a value of  $c = 0.9$  is perhaps not so unreasonable, but it can be expected to mark the upper limit. More specifically, such a high  $c$  value, when compared with crystallinity measurements of 58%, implies that the fibre phase should not be identified with

the crystalline phase. Possible alternatives are either the microfibrils or helical sections of molecule.

The second aspect of the model can be examined using the temperature dependence of the shear modulus. The shear moduli of the amorphous phase for temperatures of  $-95^\circ\text{C}$  and  $45^\circ\text{C}$  are taken to be 1.6 and 0.35 GPa, respectively. These values were obtained from dynamic torsional measurements on oriented samples<sup>25</sup>. The values quoted here are for samples of draw ratio equal to 7.6, which is assumed to mark the onset of fibril formation. Several problems arise concerning the values chosen for the shear modulus, namely the values used are macroscopic values; and although at  $-95^\circ\text{C}$  the variation of shear modulus with draw ratio is small, this is not the case at  $45^\circ\text{C}$  where the shear moduli for samples of draw ratio 3.7 and 16 are 0.15 and 0.65 GPa, respectively.

From equation (4) it can be seen that  $x$  is proportional to  $G_m^{1/2}$  so that the value of  $x$  at  $45^\circ\text{C}$  for any sample can be calculated from that at  $-95^\circ\text{C}$  and the square root of the ratio of the two shear moduli. The appropriate modulus is then calculated using equation (3). The predicted dependence of the modulus with draw ratio at this temperature is also shown in *Figure 4*. This time the agreement between the predicted and the experimental results is not quite so good with discrepancies occurring at high draw ratios. Moreover, although different values for the shear moduli can alter the slope of this curve they also change the absolute values in such a way that the overall fit is not improved. Significant improvement can be achieved, however, if the modulus of the fibrils at  $45^\circ\text{C}$  is less than that at  $-95^\circ\text{C}$ , and a slight adjustment is made to the shear moduli. This latter change is not too serious in the light of the reservations concerning the shear moduli expressed above.

Because of the large quantity of unknowns in equations (3) and (4) it is not possible to rigorously test the fibre composite model. The good agreement obtained here shows that the model cannot be excluded. However, until some of the parameters are more accurately known, its use must be considered limited.

Arridge and Barham<sup>9</sup> have used the fibre composite model to interpret the room temperature moduli of IPP but have used a considerably lower value for  $c$  of 0.58. They have also introduced a contribution to the macroscopic modulus from the matrix phase, but have not extended the model to low temperatures. Although they found good agreement between model and experiment there is still the problem of identifying the model parameters with their morphological counterparts. Like the work here, it suffers from the criticism of being a mathematical, rather than a physical exercise, although it is possible that further work may resolve this problem and give the model physical support.

## DISCUSSION

*Figure 2* shows that the mechanical behaviour is very dependent on temperature whilst the presence of the  $\beta$  relaxation at about  $20^\circ\text{C}$  for a frequency of 10 Hz is indicated by the  $\tan \delta$  curves in *Figure 3*. This relaxation is considered to be due to the onset of chain mobility in the non-crystalline phase<sup>27</sup>. It is therefore necessary to select carefully in the first instance the temperature or temperatures at which detailed mechanical modelling should be attempted. Low temperatures should provide

some simplification as the structure is then rigid and molecular orientation is likely to be the dominant factor, although it is possible that the presence of two phases is still important. A temperature of  $-95^{\circ}\text{C}$  was considered suitable for these purposes. Selection of a second temperature is not so easy because of the presence of the  $\beta$  relaxation at about room temperature but a value of  $45^{\circ}\text{C}$  was considered appropriate to include the effects of this relaxation in the mechanical response at 10 Hz. The reasonable agreement between the dynamic moduli at this temperature and the isochronal creep moduli at room temperature can be explained in terms of time/temperature equivalence.

For the rigid structure the single-phase aggregate model is remarkably successful when the crystalline compliances are used, indicating that below the  $\beta$  relaxation the mechanical behaviour of the non-crystalline phase is similar to that of the crystalline phase. As is the case with other materials, better agreement is found when Reuss averaging, rather than Voigt averaging is used. A significant improvement of this approach over previous applications of the model to other materials lies in the fact that the values for the intrinsic compliances, with one exception, ( $2s_{13} + s_{44}$ ), are more closely identified with the crystalline phase rather than being obtained from measurements on very highly oriented samples. Nevertheless, the value chosen for this one unknown parameter,  $0.41 \text{ GPa}^{-1}$ , is reasonable in the light of low temperature measurements of the shear modulus on oriented samples, whilst ultrasonic measurements of  $S_{13}$  and  $S_{44}$  at temperatures below the glass transition, carried out by Leung and Choy<sup>14</sup>, indicate a value for ( $2s_{13} + s_{44}$ ) slightly less than  $0.5 \text{ GPa}^{-1}$ . In any case, the predictions of the model are comparatively insensitive to relatively large changes in the value of this parameter.

At temperatures above the  $\beta$  relaxation the difference between the properties of the two phases becomes pronounced and consequently a single phase model would not be expected to work. The success of a two phase model, however, is perhaps better than expected, although the quality of the fit in *Figure 6* depends on the assumption of homogeneous stress in the isotropic material and the values chosen for  $s_{11}^a$  and ( $2s_{13}^a + s_{44}^a$ ). How these values relate to those of the crystal, or perhaps more specifically the non-crystalline material at low temperatures, depends on which are the most sensitive to the increased mobility of the molecules above the  $\beta$  relaxation. The best agreement in *Figure 6* is achieved when  $s_{11}^a$  is considered to be the most temperature sensitive and suggests that the reason why a two phase model is necessary above the  $\beta$  relaxation is because this relaxation significantly affects the value of  $s_{11}$  for the non-crystalline phase.

Such an explanation, however, would also suggest that the removal of the  $\beta$  relaxation through orientation would introduce an orientation dependence to the value of  $s_{11}^a$ . A consequence of this is the expectation that the modulus of a sample drawn past this stage would be relatively insensitive to changes in temperature. *Figure 3* shows that the  $\beta$  relaxation has disappeared at high draw ratios yet there is still a considerable difference between the high and low temperature moduli. This temperature dependence of the macroscopic moduli can be explained by introducing a temperature dependence to the shear component in the non-crystalline material, ( $2s_{13}^a + s_{44}^a$ ). It is not unreasonable to expect this temperature

dependence to be significant in the highly drawn samples where the structure is more regular.

It is also possible that  $s_{33}$  for both crystalline and non-crystalline material is temperature dependent. Tadaoki *et al.*<sup>28</sup> have shown that the chain modulus can fall as the temperature increases because of atomic vibrations. They showed that the lattice compliance of Kevlar 49 rose by about 25% between 300 K and 500 K. While measurements of  $s_{33}^c$  from the crystal strain experiments reported here are not accurate enough and do not cover a wide enough temperature range to exclude such a variation for IPP, they do show that there is no significant change in the apparent lattice compliance caused by crossing the  $\beta$  relaxation. This implies that there is no change in the mechanical coupling and that Reuss averaging applies above and below the  $\beta$  relaxation. Such a view is supported by the success of Reuss averaging in both the single and two phase aggregate models. Recent work in our laboratories<sup>29</sup> would suggest that  $s_{33}^c$  is temperature dependent but this may arise for the reason given by Tadaoki *et al.* and not through changes in the mechanical coupling.

Obviously, the introduction of temperature and orientation dependent intrinsic properties renders the model much more complicated but it might be possible to model the mechanical behaviour with an orientation sensitive value for  $s_{11}^a$ , so that the contribution to the macroscopic compliance from the  $s_{11}^a$  term drops for two reasons; namely the appropriate value for  $\langle \sin^4 \theta \rangle$  is low because of the high orientation; and the value of  $s_{11}^a$  has fallen because of the conformations being locked in by physical constraints, e.g. taut tie molecules. At the same time the creation of a more regular structure with increasing orientation might cause an increase in the value of ( $2s_{13}^a + s_{44}^a$ ). Thus, at a particular temperature, the mechanical improvement at high draw ratios occurs because of the removal of the  $\beta$  relaxation but the variation with temperature occurs because the sensitivity of the shear term to changes in temperature increases at high draw ratios.

The importance of shear at high draw ratios is implied by the partial success of the fibre composite analysis. For close hexagonal packing of the fibrils the agreement of the model with low temperature data is very good for draw ratios greater than 8, setting a value for the draw ratio at which transformation from spherulitic to fibrillar structure is complete. This agrees with the analysis of Peterlin<sup>30</sup>. One problem with the fibre composite model is the identification of the fibre phase and an estimation of the fibre modulus considering that measurements of crystallinity are considerably less than the value for  $c$ . If the fibre phase is identified with the morphologically distinct microfibrils, at low temperatures the moduli of the fibrils might be expected to be close to the crystal value, but at temperatures above the glass relaxation the moduli of the fibrils are more likely to be less than the crystal modulus. This change in modulus (with temperature) of the fibre phase might explain the more gradual rise in modulus at  $45^{\circ}\text{C}$  than is predicted from the fibre composite model.

Recent work by Taraiya *et al.*<sup>11</sup> suggests that stacked lamellae in highly oriented polypropylene are bridged by a combination of disordered crystallites and taut tie molecules. Although this particular intercrystalline bridge model is not the same as that discussed for oriented polyethylene<sup>10</sup> it is interesting to note that at the



conformational level there is no distinction between taut tie molecules and the molecules in disordered or conventional polypropylene crystallites, the molecules all adopting the  $3_1$  conformation. This, together with the comparative success of the fibre composite model, raises the interesting possibility that the fibre phase might be identified with stereoregular sequences of  $3_1$  IPP.

## CONCLUSIONS

The mechanical behaviour of isotactic polypropylene at low temperatures has been shown to be independent of the morphology and can be predicted by a single phase aggregate model using measurements of the overall orientation and the intrinsic mechanical properties of the crystalline phase. The aggregate model has also proved successful above the  $\beta$  relaxation when the crystalline and non-crystalline phases are considered separately. The major surprise is the success of Reuss averaging both above and below the  $\beta$  relaxation. This situation is given support by the fact that little change in the apparent crystal modulus is observed on crossing this relaxation. The disappearance of the  $\beta$  relaxation in highly drawn samples leads to an increase in modulus possibly through a change in the lateral compliance value  $s_{11}^a$ . The temperature dependence of the moduli of these highly drawn samples depends on the greater temperature sensitivity of the shear term when the  $\beta$  relaxation has been removed. The importance of shear is seen from the partial success of the fibre composite model. Above a draw ratio of about 8, mechanical improvement may be achieved by increasing the reinforcing effect of a fibre phase. If the fibre phase is identified with the fibrillar structure this may be achieved through an increase in the fibril moduli, caused by an increase in tie molecules, as well as through changes in the aspect ratio and matrix shear modulus. Alternatively, it is possible that the fibre phase may be sections of stereoregular molecule in the  $3_1$  helical conformation, in which case a greater reinforcement may be produced by removal of kinks in the chains.

## REFERENCES

- 1 Takayanagi, M., Imada, K. and Kajiyama, T. *J. Polym. Sci. C* 1966, **15**, 263
- 2 Ward, I. M. *Proc. Phys. Soc.* 1962, **80**, 1176
- 3 Pinnock, P. R. and Ward, I. M. *Br. J. Appl. Phys.* 1966, **17**, 575
- 4 Hadley, D. W., Pinnock, P. R. and Ward, I. M. *J. Mater. Sci.* 1969, **4**, 152
- 5 Williams, T. J. *J. Mater. Sci.* 1973, **8**, 59
- 6 Chan, O. K., Chen, F. C., Choy, C. L. and Ward, I. M. *J. Phys. D.* 1978, **11**, 617
- 7 Barham, P. J. and Arridge, R. G. C. *J. Polym. Sci., Polym. Phys. Edn.* 1977, **15**, 1177
- 8 Arridge, R. G. C. and Barham, P. J. *Polymer* 1978, **19**, 654
- 9 Arridge, R. G. C. and Barham, P. J. *J. Polym. Sci., Polym. Phys. Edn.* 1978, **16**, 1297
- 10 Gibson, A. G., Davies, G. R. and Ward, I. M. *Polymer* 1978, **19**, 683
- 11 Taraiya, A. K., Unwin, A. P. and Ward, I. M. *J. Polym. Sci., Polym. Phys. Edn.* 1988, **26**, 817
- 12 Seferis, J. C., McCullough, R. L. and Samuels, R. J. *J. Macromol. Sci. Phys.* 1977, **B13**, 357
- 13 Seferis, J. C. and Samuels, R. J. *Polym. Eng. Sci.* 1979, **19**, 975
- 14 Leung, W. P. and Choy, C. L. *J. Polym. Sci., Polym. Phys. Edn.* 1981, **20**, 1
- 15 Yamada, K., Kamezawa, M. and Takayanagi, M. *J. Appl. Polym. Sci.* 1981, **26**, 49
- 16 Unwin, A. P., Bower, D. I. and Ward, I. M. *Polymer* 1985, **26**, 1605
- 17 Yamada, A. G., Jawad, S. A., Davies, G. R. and Ward, I. M. *Polymer* 1982, **23**, 349
- 18 Gupta, V. B. and Ward, I. M. *J. Macromol. Sci. Phys.* 1967, **B1**, 373
- 19 Rushworth, A. *PhD Thesis*, Leeds University, 1977
- 20 Troughton, M. J., Davies, G. R. and Ward, I. M. *Polymer* 1989, **30**, 58
- 21 Sakurada, I. and Kaji, K. *J. Polym. Sci. C* 1970, **31**, 57
- 22 Fanconi, B. and Rabolt, J. F. *J. Polym. Sci., Polym. Phys. Edn.* 1985, **23**, 120
- 23 Tashiro, K., Kobayashi, M. and Tadokoro, T. *Macromolecules* 1977, **10**, 731
- 24 Sakurada, I., Ito, T. and Nakamae, K. *J. Polym. Sci. C* 1966, **15**, 75
- 25 Jawad, S., private communication
- 26 Luisi, P. L. *Polymer* 1972, **13**, 232
- 27 McCrum, N. G., Read, B. E. and Williams, G. 'Anelastic and Dielectric Effects in Polymeric Solids', Wiley, New York, 1967, p. 377
- 28 Tadaoki, I., Tashiro, K., Kobayashi, M. and Tadokoro, H. *Macromolecules* 1987, **20**, 347
- 29 Duxbury, J. *PhD Thesis*, Leeds University, 1986
- 30 Peterlin, A. *Colloid Polym. Sci.* 1975, **253**, 809